



Letters

Constraints on fluid origins and migration velocities along the Marmara Main Fault (Sea of Marmara, Turkey) using helium isotopes

P. Burnard ^{a,*}, S. Bourlange ^{a,b}, P. Henry ^c, L. Geli ^d, M.D. Tryon ^e, B. Natal'in ^f, A.M.C. Sengör ^f, M.S. Özeren ^f, M.N. Çagatay ^f

^a CRPG-CNRS, BP 20, 54501 Vandoeuvre-lès-Nancy Cedex, France

^b Université de Lorraine, CRPG (UPR2300), Vandoeuvre-lès Nancy, 54501, France

^c CEREGE, Aix-Marseille Université, CNRS, Collège de France, BP 80, 13545 Aix en Provence Cedex 04, France

^d Ifremer, Marine Geosciences Department, 29280 Plouzané, France

^e Scripps Institution of Oceanography, La Jolla, CA 92093-0244, USA

^f Istanbul Technical University, Faculty of Mines, Geology Department, Maslak, 34469 Istanbul, Turkey

ARTICLE INFO

Article history:

Received 22 November 2011

Received in revised form

23 May 2012

Accepted 25 May 2012

Editor: T.M. Harrison

Keywords:

fluids

gas emission

helium

Marmara Sea

North Anatolian Fault

ABSTRACT

Fluids venting from the submarine portion of the Marmara Main Fault (part of the North Anatolian Fault system, Turkey) were sampled in Ti bottles deployed by submersible. The fluids consist of mixtures of fault derived gases, fault related cold seep fluids, and ambient seawater; these components can readily be distinguished using the isotopes of He and the He/Ne ratios. ${}^3\text{He}/{}^4\text{He}$ ratios range between 0.03 ± 0.1 and 4.9 ± 0.4 Ra, indicating that both crustal and mantle derived sources of helium are sampled by the fault. The dominant gas in all the samples analyzed is methane with the abundance of CO_2 below detection ($\leq 2\%$) in the mantle rich (high ${}^3\text{He}/{}^4\text{He}$) fluids. This is in contrast to nearly all mantle derived fluids where the C species are dominated by CO_2 . While high CH_4/CO_2 ratios may reflect organic or inorganic reactions within the crust which reduce mantle derived CO_2 to methane, this is not *a priori* necessary: we show that simple dilution of mantle fluids with methane produced within local sediments could result in the high ${}^3\text{He}/{}^4\text{He}$, methane rich gases currently emanating from the fault. This observation is supported by an anticorrelation between ${}^3\text{He}/{}^4\text{He}$ and $\text{C}^{3\text{He}}$, which is consistent with addition of C and ${}^4\text{He}$ simultaneously to the fluids.

The highest ${}^3\text{He}/{}^4\text{He}$ ratios were found in the Tekirdag Basin, at the foot of the escarpment bordering the Western Sea of Marmara, where seismic data are consistent with the presence of a fault network at depth which could provide conduits permitting deep-seated fluids to rise to the surface. The lack of recent volcanism, or any evidence of underlying magmatism in the area, along with low temperature fluids, strongly suggests that the ${}^3\text{He}$ -rich helium in these fluids was derived from the mantle itself with the Marmara Main Fault providing a high permeability conduit from the mantle to the surface. Assuming that the mantle source to the fluids originally had a ${}^3\text{He}/{}^4\text{He}$ ratio of 6 Ra, the minimum fluid velocities (considering only vertical transport and no mixing with parentless ${}^4\text{He}$) implied by the high ${}^3\text{He}/{}^4\text{He}$ ratios are of the order of $1\text{--}100 \text{ mm yr}^{-1}$.

© 2012 Elsevier B.V. All rights reserved.

1. Introduction

Since Kennedy et al. (1997) demonstrated that mantle derived He emanates from the San Andreas Fault, the He isotopic composition of fault-related fluids of numerous different faults has shown that volatiles escape the mantle via crustal pathways (faults) to the surface. This in turn implies the existence of high permeability passages that cross both the mantle–crust boundary and the ductile lower crust. The isotopes of He are ideally suited

for tracing these mantle derived fluids at the Earth's surface due to two fortunate circumstances: firstly, the mantle retains isotopically distinct primordial He and, secondly, He concentrations in surface waters are extremely low (He is not retained in the atmosphere and is insoluble in aqueous fluids). As a result, trace inputs of He from the deep earth can readily be identified at the surface, and the source of this He (mantle or crust) can be identified from He isotope measurements.

Frequently, release of mantle He is associated with magmatism and it seems logical that the mantle must melt in order to liberate He (diffusion through solid mantle being too slow to account for the observed fluxes). Escape of mantle-derived He in zones of extension that do not have any obvious association with

* Corresponding author.

E-mail address: peteb@crpg.cnrs-nancy.fr (P. Burnard).

active volcanism is well known (Brauer et al., 2009; Crossey et al., 2009; Kennedy and Van Soest, 2007; Kulogoski et al., 2005; Oxburgh and O'Nions, 1987). These areas (The Eger Rift, Hungary, The Basin and Range province, USA, the Morongo Groundwater Basin, USA, The Pannonian Basin, Hungary) are characterized by high heat flow, thin crust and possible magmatism at depth ('underplating') hence it is not surprising that mantle He percolates to the surface.

The presence of mantle He in regions of active compression not associated with magmatism is less common and more difficult to reconcile with fluid (He) transfer between mantle and shallow crust. Regions of compression/strike-slip faulting are not associated with thinned crust (frequently the reverse) or with heat flow anomalies which might indicate recent underplating by mantle melts. Thus it is difficult to understand how the mantle underlying the fault liberates He (and presumably other volatiles), or how the released volatiles traverse several kms of ductile lower crust. Nevertheless, $\geq 50\%$ of the He along some sections of the San Andreas Fault (SAF), of the Niigata-Kobe tectonic zone and of the North Anatolian Fault is derived from the mantle (Gulec and Hilton, 2006; Gulec et al., 2002; Kennedy et al., 1997; Mutlu et al., 2008; Umeda et al., 2008). Occurrences of such high fractions of mantle He along these faults are in general limited to restricted sections of fault and that, for the most part, these faults are characterized by significantly lower proportions of mantle He (typically 10–20%) in contrast to the more studied higher $^3\text{He}/^4\text{He}$ localities.

The presence of mantle fluids in faults could also have implications for the faults themselves: the lack of a thermal anomaly on these strike-slip faults is suggestive of low frictional strength (Lachenbruch and Sass, 1980; Zoback and Beroza, 1993) which is inconsistent with the thermomechanical properties of the fault materials. The effective shear stress required for fault slip can be greatly reduced by the presence of high pressure pore fluids. It has been hypothesized that mantle derived fluids could provide a mechanism for weakening strike slip faults (Iio et al., 2002; Kennedy et al., 1997), although calculations suggest the mantle cannot provide sufficient volatiles (Faulkner and Rutter, 2001).

Frequent fluid emissions have been observed on the seafloor of the Sea of Marmara (Géli et al., 2008) closely related to the location of the Marmara Main Fault (MMF), the western extension of the North Anatolian Fault. Thus, the MMF presents an ideal location to study the nature of fault related fluids. Here, we report new data on helium isotopes and concentrations in fluids sampled from the Sea of Marmara. Combined with previous work

(Dogan et al., 2009; Gulec and Hilton, 2006; Gulec et al., 2002; Mutlu et al., 2008), the present study provides new insights on the origin of mantle helium in the Western Marmara area.

1.1. Marmara geology and previous work on the NAF

The North Anatolian Fault (NAF) zone in Northern Turkey is a major transform plate boundary that has produced devastating historical earthquakes along its 1200 km length (Ambraseys and Jackson, 2000; Barka, 1992; Sengör et al., 2005). West of Bolu the fault divides into two main strands, the most active being the northern branch between the Gulf of Izmit and Şarköy (Sea of Marmara). The Sea of Marmara is composed of 1000 m deep basins (from east to west: the Çinarçık Basin, the Central Basin and the Tekirdag Basin), separated by two bathymetric highs orientated NE-SW, the Central and Western highs (Fig. 1). Free gas emissions in the Sea of Marmara are common and appear to be influenced by earthquake occurrence (Kuscu et al., 2005). In deeper parts, gas emissions are commonly observed along or near active faults (Armijo et al., 2005; Géli et al., 2008; Zitter et al., 2008). Chemical analysis indicates that the gas is mainly methane, and has two different origins: (1) biogenic in the Çinarçık Basin origin, and (2) thermogenic in the Western and Central Highs, probably originating from Thrace Basin (Bourry et al., 2009).

On the western slope of the Tekirdag Basin (Fig. 1), numerous densely spaced acoustic anomalies were observed rising from the sea bottom (Géli et al., 2008). Based on Ocean Bottom Seismometer (OBS) recordings, clusters of microseismicity were also documented below the western slope of the Tekirdag Basin, suggesting that tectonic strain contributes to maintaining high permeability in fault zones and that the fault network may provide conduits for deep-seated fluids to rise up to the seafloor (Tary et al., 2011). Both observations support the hypothesis that gas is probably leaking from Thrace Basin reservoirs into the Sea of Marmara, following conduits along faults, active or inactive.

The Thrace basin is an active gas and oil-producing province in Western Turkey, with well-studied geology (Perincek, 1991; Siyako and Huvaz, 2007; Turgut and Eseller, 2000), geophysics (Goncuoglu et al., 2000; Huvaz et al., 2007) and geochemistry (Coskun, 1997, 2000; Gürgey, 2009; Gürgey et al., 2005; Hosgörmez et al., 2005; Şen et al., 2009). The Late Cretaceous-Early Eocene Tethyan evolution of Western Turkey is related to subduction, ophiolite obduction and collision (Okay et al., 2001; Sengör and Yilmaz, 1981). Two major characteristics are of

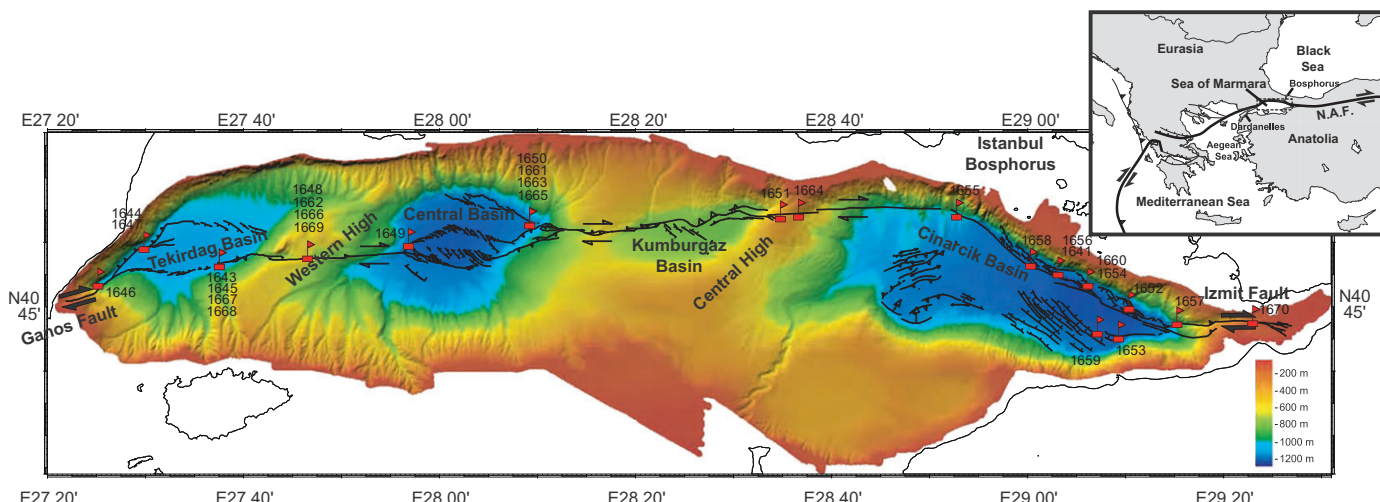


Fig. 1. Sample locations on a bathymetric map of the northern section of the Sea of Marmara. The yellow circle shows the location of well M67 where Dogan et al. (2009) report $^3\text{He}/^4\text{He}$ ratios up to 4.8 Ra.

relevance here: (1) the western NAF roughly follows the Intra-Pontide suture zone and (2) the NAF within the Sea of Marmara cross-cuts hydrocarbon gas reservoirs from the Thrace Basin gas province.

1.1.1. Helium and carbon in fault-associated fluids from western Turkey

Helium isotopes measured in geothermal emissions from the subaerial NAF in western Turkey show a wide range, from radiogenic (${}^3\text{He}/{}^4\text{He} = 0.05 \text{ Ra}$) to mantle-like (de Leeuw et al., 2010; Dogan et al., 2009; Gulec and Hilton, 2006; Gulec et al., 2002; Mutlu et al., 2008). However, the highest ratios ($> 5 \text{ Ra}$) are closely associated with active or recent volcanism mostly in eastern Anatolia and likely reflect magmatic inputs (Gulec and Hilton, 2006). There are elevated ${}^3\text{He}/{}^4\text{He}$ ratios in western and central Anatolia (e.g. at Tuzla, ${}^3\text{He}/{}^4\text{He} = 1.4 \text{ Ra}$), which are also associated with volcanic activity (Mutlu et al., 2008). As such, these mantle-like He isotopic compositions are probably not fault-related fluids per se.

At the western extremity of the NAF, i.e. between 32°W and the Sea of Marmara, the range of ${}^3\text{He}/{}^4\text{He}$ is more limited; ${}^3\text{He}/{}^4\text{He}$ ratios fall between 0.3 and $\sim 1 \text{ Ra}$. While some mantle He is present in these fault-associated fluids, this is never greater than $\sim 20\%$. However, there are two localities which have higher mantle contributions (Mudurnu and the Tekirdag/Sarkoy region) (de Leeuw et al., 2010; Dogan et al., 2009; Gulec and Hilton, 2006; Gulec et al., 2002; Mutlu et al., 2008), described below.

Mudurnu, an 80 m deep well located south of the main NAF trace (see Dogan et al. (2009) for location), had ${}^3\text{He}/{}^4\text{He} = 4.8 \text{ Ra}$ prior to 1995 (Ercan et al., 1995) but which fell to a value of 2.8 Ra in 2009. Fluid samples from the Gazikoy–Saros Fault (the on-land trace of the Marmara Main Fault) contained ca. 70% mantle He

(${}^3\text{He}/{}^4\text{He} = 4.8 \text{ Ra}$) (Dogan et al., 2009), this despite the fact that there is no significant associated recent volcanism in the region that could provide a potential magmatic source for the high ${}^3\text{He}/{}^4\text{He}$ ratios (Pe-Piper and Piper, 2007).

Carbon isotope compositions and $C/{}^3\text{He}$ ratios indicate that the C accompanying this He is predominantly of crustal origin (de Leeuw et al., 2010; Dogan et al., 2009; Gulec et al., 2002). In general, the “carrier gas” for mantle He is CO_2 , and $C/{}^3\text{He}$ ratios of mantle fluids are relatively constant at 2×10^9 ($\pm 50\%$) (Marty and Jambon, 1987). $C/{}^3\text{He}$ ratios in western Anatolia vary from mantle-like ratios to values much (10^5 times) higher, a feature commonly observed in hydrothermal fluids not directly related to volcanic activity (e.g. Japan, Western USA, Italy) (Gherardi et al., 2005; Kennedy and Van Soest, 2007; Umeda et al., 2007b). These elevated $C/{}^3\text{He}$ ratios result from a combination of phase separation and addition of C from the crust (by dissolution of carbonates or degradation of organic C) (de Leeuw et al., 2010; Gulec and Hilton, 2006).

2. Sample descriptions

A total of 31 fluid (gas+seawater) samples from the Sea of Marmara were analyzed, 26 from within basins and 5 from topographic highs; Sampling locations are shown in Fig. 1, and their locations and descriptions are provided in Table 1.

The majority of samples targeted fluid emission sites that had previously been identified using acoustic techniques (Géli et al., 2008). In some locations, active fluid activity was identified via streams of methane bubbles rising from the seafloor. More commonly, fluid presence was indicated by black reduced sediments and microbial mats on the sea floor with only minor or (more commonly) without visible fluid flow. One exceptional site,

Table 1
Sample locations and descriptions.

Sample Name	Region	Comment	Lat	Long
1645-2	Terkidag basin	Jack the smoker (incorrectly deployed) ^a	N40°48.197	E27°37.800
1645-3	Terkidag basin	Jack the smoker (incorrectly deployed) ^a	N40°48.197	E27°37.799
1647-5	Terkidag basin	Boris' Bubblers (see text for description)	N40°50.046	E27°30.206
1647-6-1	Terkidag basin	Boris' Bubblers (see text for description)	N40°50.046	E27°30.206
1647-6-2-b	Terkidag basin	Boris' Bubblers (see text for description)	N40°50.046	E27°30.206
1647-7-b	Terkidag basin	Ambient seawater in the vicinity of Boris' Bubblers	N40°50.046	E27°30.206
1649-5	Central Basin	Bubbling vent in black mat	N40°49.936	E27°56.044
1649-6-b	Wedge of central basin	Bubbles escaping sedimented sea floor	N40°49.529	E27°56.032
1649-7-a	Wedge of central basin	Bubbles escaping sedimented sea floor	N40°49.529	E27°56.032
1650-2	Central Basin	Fluid from a small black chimney in the center of a black patch	N40°51.488	E28°9.529
1650-2-a	Central Basin	Fluid from a small black chimney in the center of a black patch	N40°51.488	E28°9.529
1650-3	Central Basin	Fluid from a small black chimney in the center of a black patch	N40°51.488	E28°9.529
1651-6-A	E of Kumburgaz Basin	Black patch with bacterial mat	N40°52.093	E28.35.028
1653-5-a	S Slope Cinarcik Basin	Black patch close to a carbonate crust	N40°42.300	E29°9.360
1653-6-a	S Slope Cinarcik Basin	Large black patch	N40°42.720	E29°10.080
1653-7-a	S Slope Cinarcik Basin	Large black patch	N40°42.720	E29°10.080
1653-8-a	S Slope Cinarcik Basin	Large black patch	N40°42.720	E29°10.080
1654-4-a	N Scarp Cinarcik Basin	Black patch	N40°46.803'	E29°06.231'
1655-c4	Central Basin	Bubbles within a push core	N40°52.567	E28°51.230
1658-c2	Cinarcik Basin	Bubbles within a push core	N40°48.578	E29°0.502
1659-1	Cinarcik Basin	Bubbles escaping black mat	N40°42.991	E29°6.991
1659-2	Cinarcik Basin	Bubbles escaping black mat	N40°42.994	E29°6.976
1659-3	S Slope Cinarcik Basin	Bubble stream	N40°46.803'	E29°06.231'
1659-4-a	S Slope Cinarcik Basin	Bubble stream	N40°46.803'	E29°06.231'
1662-2-1	Western High	Bubbling stream above carbonated chimney	N40°49.071	E27°46.822
1662-2-2	Western High	Bubbling stream above carbonated chimney	N40°49.071	E27°46.822
1662-c1	Western High	Bubbles within a push core	N40°49.063	E27°46.829
1662-c2	Western High	Bubbles within a push core	N40°49.063	E27°46.829
1664-2	Cinarcik Basin	Inverted-funnel gas sample of gas streaming from small (cm-sized) chimneys	N40°51.710	E28°46.006
1664-3 bis 1	Cinarcik Basin	Bubbling stream above carbonated chimney	N40°51.710	E28°35.006
1664-4-1 bis	Central High	Bubbling stream above carbonated chimney	N40°51.611	E28°34.979

^a These two samples were not given sufficient time to aspirate the fluids into the Ti bottle.

known as “Boris’ Bubblers”, (“BB”, after Boris Natal’in, the discoverer; Fig. 1) had several vigorous bubble streams emanating from the intersection of the two faults. One of these is a NE-trending splay of the Ganos Thrust which probably represents the Intra-Pontide suture. This fault is cut by an E–W-trending dextral fault which is a splay of the North Anatolian fault. From a cluster of shallow (< 7 km depth) microseismicity Tary et al. (2011) identified predominantly normal movement in the immediate vicinity of BB on a fault oriented NW–SE; the fault orientation and mechanism can be correlated with a series of normal on-land faults in the Ganos mountains (Okay et al., 1999). BB is located on the northern wall of the dextral fault. Methane bubble streams are emitted from tectonically controlled tension gashes, associated with dextral displacement along the E–W fault cutting the late Cretaceous–Paleocene Intra-Pontide suture.

None of the fluid emission sites was associated with a temperature anomaly: fluid temperatures were in the range $14 \pm 1^\circ\text{C}$, consistent with previous work in the region (Zitter et al., 2008).

3. Sampling and analytical methods

All fluids analyzed in this study were sampled from the seafloor using specially constructed samplers. The sampler consisted of a Ti bottle of ca. 200 cc capacity connected to a capillary tube (0.5 mm diameter) via a vacuum valve. On board ship (< 12 h prior to sampling) the bottle was evacuated to $< 10^{-3}$ mbar; the samplers

retained this vacuum until deployed on the seafloor. Then, once positioned above the site on the seafloor, fluid was aspirated into the Ti bottle (through the capillary tube) by the vacuum in the bottle. The bottle contents remained at seafloor pressure (the valve was sufficient to seal the bottle). Temperature sensors recorded the temperature adjacent to the capillary tube. Four Ti bottles were available per *Nautile* dive.

Once on board, the contents of the Ti bottle were immediately degassed by transferring the mixture of gases and gas-saturated seawater into an evacuated ($< 10^{-5}$ mbar) volume of ~ 2000 cm³ following Jean-Baptiste et al. (1991). Care was taken to ensure that all air was pumped out of transfer pipes between the Ti tube and the expansion volume. After ca. 15 min, the liquid had completely degassed (via the fine jet by which it entered the expansion volume); compressing large bellows on the expansion volume concentrated the sample by a factor of 4. The headspace gases were sealed in four copper pinch-off tubes providing 4 replicates of the gases dissolved in each Ti bottle sample of seawater. The pressure in the Cu tubes at the time of sampling is noted in Table 2.

The copper tubes were returned to the Noble Gas Laboratory at CRPG, Nancy. The tubes were opened under vacuum and the gas samples purified using hot and cold Ti sponge getters and separated from the heavy noble gases using liquid nitrogen cooled activated charcoal. The remaining He and Ne were expanded into a Helix SFT Multicollector noble gas mass spectrometer for He and Ne analysis. Blanks were negligible compared to the samples. The system was calibrated with respect to an air standard which

Table 2
Gas contents and noble gas compositions.

Sample name	P (mbar)	ΣC (mol $\times 10^{-6}$)	^4He (mol $\times 10^{-12}$)	$^3\text{He}/^4\text{He}$ (Ra)	$^4\text{He}/^{20}\text{Ne}$	$^3\text{He}/^4\text{He}^*$ (Ra)	$[^3\text{He}]^a$ (mol g ⁻¹ $\times 10^{-12}$)	$C/^3\text{He}^b \times 10^9$
1645-2	78.5	13.3	10 ± 0.4	1 ± 0.1	0.4 ± 0.03	–	0.58 ± 0.06	946 ± 134
1645-3	36	–	0.73 ± 0.03	1 ± 0.3	0.91 ± 0.07	1.0 ± 0.3	0.09 ± 0.03	–
1647-5	904	271	753 ± 29	4.3 ± 0.2	1.8 ± 0.1	4.9 ± 0.4	16 ± 1	60 ± 7
1647-6-1	1366	416	12531 ± 479	4.4 ± 0.6	102 ± 7	4.4 ± 0.7	180 ± 25	5 ± 1
1647-6-2-b	721	214	23.7 ± 0.5	4.6 ± 0.2	41 ± 6	4.6 ± 0.7	0.67 ± 0.03	1402 ± 152
1647-7-b	43.8	2.4	9.7 ± 0.2	1.02 ± 0.04	0.33 ± 0.05	–	1.00 ± 0.04	174 ± 19
1649-5	27	–	1.93 ± 0.07	1.2 ± 0.2	1.7 ± 0.1	1.2 ± 0.2	0.38 ± 0.05	–
1649-6-b	33	–	0.88 ± 0.02	0.94 ± 0.03	0.35 ± 0.03	–	0.111 ± 0.004	–
1649-7-a	33	–	1.89 ± 0.04	0.96 ± 0.04	0.23 ± 0.01	–	0.24 ± 0.01	–
1650-2	82	14	8.9 ± 0.3	1 ± 0.1	0.29 ± 0.02	–	0.47 ± 0.06	1151 ± 179
1650-2-a	82	14	5.9 ± 0.1	0.99 ± 0.04	0.33 ± 0.02	–	0.32 ± 0.01	1754 ± 193
1650-3	51.32	4.8	15.7 ± 0.6	1.16 ± 0.08	0.31 ± 0.02	–	1.6 ± 0.1	187 ± 23
1651-6-A	27.5	–	2.83 ± 0.07	1.08 ± 0.04	0.39 ± 0.06	–	0.49 ± 0.02	–
1653-5-a	31	–	0.8 ± 0.02	0.93 ± 0.03	0.32 ± 0.02	–	0.11 ± 0.00	–
1653-6-a	31.5	–	1.61 ± 0.03	0.95 ± 0.03	0.23 ± 0.02	–	0.21 ± 0.01	–
1653-7-a	30.5	–	0.83 ± 0.02	0.89 ± 0.03	0.71 ± 0.06	0.81 ± 0.07	0.11 ± 0.00	–
1653-8-a	28.4	–	1.34 ± 0.03	0.03 ± 0.01	0.26 ± 0.02	–	0.01 ± 0.00	–
1654-4-a	29	–	2.71 ± 0.06	1.09 ± 0.04	0.45 ± 0.06	1.24 ± 0.18	0.45 ± 0.02	–
1655-c4	564.5	165	531 ± 20	0.95 ± 0.06	0.25 ± 0.02	–	4.0 ± 0.3	234 ± 29
1658-c2	1000	301	1033 ± 40	1.02 ± 0.05	0.25 ± 0.02	–	4.7 ± 0.3	204 ± 24
1659-1	160	39	10 ± 0.4	0.8 ± 0.3	0.75 ± 0.05	0.64 ± 0.21	0.21 ± 0.07	3457 ± 1182
1659-2	96.46	19	13 ± 0.5	0.87 ± 0.09	0.35 ± 0.02	–	0.52 ± 0.06	1191 ± 176
1659-3	44	–	7.5 ± 0.2	0.96 ± 0.03	0.24 ± 0.03	–	0.73 ± 0.03	–
1659-4-a	46.8	–	7.3 ± 0.2	0.97 ± 0.03	0.21 ± 0.03	–	0.67 ± 0.03	–
1662-2-1	1181	358	248 ± 9	0.07 ± 0.03	9.5 ± 0.7	0.04 ± 0.02	0.06 ± 0.03	14721 ± 6259
1662-2-2	1333	405	271 ± 10	0.05 ± 0.04	25 ± 2	0.04 ± 0.03	0.05 ± 0.03	21364 ± 15419
1662-c1	1005	303	1840 ± 70	0.9 ± 0.1	0.13 ± 0.01	–	7.1 ± 0.9	131 ± 21
1662-c2	705	209	1308 ± 50	1.08 ± 0.06	0.67 ± 0.05	1.14 ± 0.10	8.9 ± 0.6	106 ± 13
1664-2	1236	375	1686 ± 64	0.28 ± 0.05	45 ± 3	0.28 ± 0.05	1.7 ± 0.3	567 ± 114
1664-3 bis 1	1409	429	127634 ± 4883	0.41 ± 0.01	348 ± 229	0.41 ± 0.27	163 ± 9	6 ± 1
1664-4-1 bis	1279	388	1609 ± 62	0.43 ± 0.05	193 ± 21	0.43 ± 0.07	2.4 ± 0.3	401 ± 66

^a $^3\text{He}/^4\text{He}$ corrected for atmospheric contribution following Sano and Wakita (1985); Samples with a “–” are too contaminated with air to calculate an air-corrected $^3\text{He}/^4\text{He}$ ratio.

^b $C/^3\text{He}$ concentrations are those in the (water dominated) fluid sampled by the Ti bottle sampler.

^b $C/^3\text{He}$ ratios are for the gases that degassed from the Ti bottle sampler (see text for detail). Samples with a “–” did not contain any gas in excess of air dissolved in seawater.

delivered 7.37×10^{-12} mol ${}^4\text{He}$ and 2.56×10^{-11} mol ${}^{20}\text{Ne}$. Uncertainties (1 sigma) are calculated by quadratic propagation of measurement errors, uncertainties in blanks and the uncertainty of at least ten standards intercalated with samples.

The major gas composition (total carbon species) of one copper tube sampled at BB was analyzed in the Stable Isotope Laboratory of CRPG.

4. Results

4.1. Helium concentrations and isotopes

The He isotope data along with He/Ne ratios and tube pressures are reported in Table 2; He concentrations reported in Table 2 are their concentrations in the fluids as sampled by the Ti bottles (i.e. seawater and excess gases). The C/He ratios in the Cu tubes (which contain only the gases that were exsolved from the Ti bottles) can be calculated by converting the pressure within the Cu tube into moles as the volumes of the Cu tubes are known. The pressures measured were corrected for the contribution of dissolved and excess atmospheric noble gases in seawater ($890 \pm 36 \mu\text{mol L}^{-1}$ (Tanaka and Watanabe, 2007) and for the partial vapor pressure of water (23.3 mbar at 20 °C); some samples do not contain resolvable additional gases. For the samples recording pressures over and above the seawater gas+vapor pressure of water ($=36.1 \pm 7.8$ mbar), the C/ ${}^3\text{He}$ ratios are given in Table 2. C/ ${}^3\text{He}$ ratios are calculated assuming that the gas phase is entirely composed of CH₄, consistent with analyses of Marmara Sea fluids although the major gas composition was not measured in all the fluids. However, uncertainties in the major fluid composition are unlikely to significantly affect the C/ ${}^3\text{He}$ ratios calculated this way considering that the fluids are dominated by either CH₄ or CO₂.

A significant number of samples (17 samples representing 10 different locations; Fig. 2; Table 2) have ${}^3\text{He}/{}^4\text{He}$ ratios close to 1 Ra and low He/Ne. The helium trapped in these samples is indistinguishable from atmospheric He, i.e. either pure seawater noble gases were sampled or else atmospheric contamination overwhelmed the sample He. There is no evidence for solid-earth He (mantle or crustal) in these low He/Ne samples. Of the samples that do contain solid-earth He (14 samples) all but two (1653-8 and 1662-2, Western High) contain identifiable mantle He inputs, for the most part about 20% of the He is of mantle origin. However, the samples from Boris' Bubblers (Dive 1647) are clearly different with ${}^3\text{He}/{}^4\text{He}$ ratios of 4.3–4.6 Ra which implies that ca. 70% of the He originated in the mantle. There is no readily discernable gradient or geographic pattern in ${}^3\text{He}/{}^4\text{He}$ along the MMF.

4.2. Major gas compositions

The major gas composition is available for four sites, 1659, 1662, 1664 (Bourry et al., 2009) and 1647 (on a Cu tube; this study). All the gases essentially consist of methane with trace amounts of CO₂ and C₂+C₃ hydrocarbons.

4.3. C/ ${}^3\text{He}$ ratios

The C/ ${}^3\text{He}$ ratios calculated from the pressure of gas degassed from the Ti bottle samples (see above; Table 2) are in the 1×10^9 – 2×10^{13} range, consistent with previously recorded C/ ${}^3\text{He}$ ratios along the NAF (de Leeuw et al., 2010; Dogan et al., 2009; Mutlu et al., 2008).

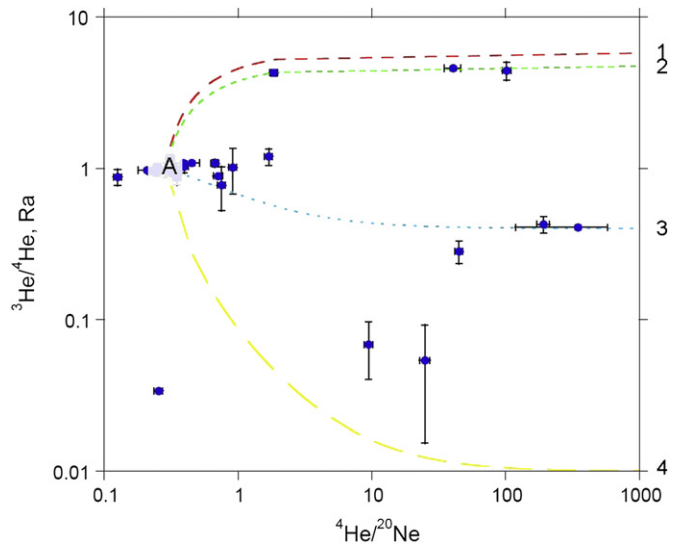


Fig. 2. He isotope and ${}^4\text{He}/{}^{20}\text{Ne}$ ratio for fluids associated with faulting in the Sea of Marmara. The wide range in He isotopic compositions and in He/Ne ratios can be explained in terms of mixing between 3 sources of helium: atmospheric, mantle-derived and radiogenic He produced in the crust. Illustrative mixing curves are shown for mixing with different geological fluid endmembers, fluid 1 being a pure mantle endmember (${}^3\text{He}/{}^4\text{He}=6$ Ra) (Gautheron and Moreira, 2002; Moreira et al., 1998); fluids 2 and 3 are mantle/crustal fluid mixtures with 70% and 20% mantle He contributions respectively ($({}^3\text{He}/{}^4\text{He})_{\text{Fluid2}}=4.9$ Ra, corresponding to the source of BB fluids; see text for further details); fluid 4 is a pure crustal fluid with ${}^3\text{He}/{}^4\text{He}=0.01$ Ra. With the exception of one analysis (1653-8-a) all the data can be explained by mixing between these fluids (some of the He/Ne variation may also be due to fluid-gas fractionation during bubble formation on the seafloor (Holzner et al., 2008)). The composition of 1653-8-a is thought to be an analytical artifact resulting from a Cu pinch off tube that was incorrectly sealed such that He escaped from the tube but not Ne (tests on Cu pinch off tubes have confirmed this as a potential mechanism).

5. Discussion

We clearly identify the presence of He from the mantle in the majority of the high He/Ne samples (Fig. 2). For the most part, MMF fluids contain ~20% mantle He. It seems likely that this “background” mantle He signature results from a porous MOHO allowing leakage of mantle He into the crust. The fact that the contribution of mantle derived He is geographically homogeneous with no apparent trend along the fault suggests that the process accounting for mantle He in these fluids has a long wavelength (> 500 km). A “leaky MOHO” possibly resulting from the trans-tensional regime of the Sea of Marmara and its surroundings (Sengör et al., 2005) would be consistent with the geographically homogeneous He isotope distribution. By contrast, discrete intrusions created by underplating (which could also result in a ${}^3\text{He}$ flux) would result in a more heterogeneous He isotope distribution along the MMF and NAF, and would result in high heat flows (which are not observed in this area). This is consistent with similar observations in extensional regimes (Kennedy and Van Soest, 2007; Kulangoski et al., 2005), where a leaky MOHO is thought to be the origin of a mantle He flux to the surface.

The sample from the Western High, 1662-2, is the only sample where mantle ${}^3\text{He}$ is certainly absent. Pore fluids from this location have exceptionally high Li concentrations, probably from high temperature water rock interactions (Tryon et al., 2010). Plausibly, the radiogenic He coupled with elevated Li at this location is the result of alteration of basement rocks.

The extremely active site of Boris' Bubblers is clearly different: up to 70% mantle He was found in the BB samples (Fluid 2 in Fig. 2). Similar quantities of mantle-derived He have been observed on the nearby on-land Gazikoy–Saros Fault (Tekirdag)

by Dogan et al. (2009), essentially from the onshore equivalent of the splay fault where Boris' Bubblers is situated (Fig. 1). A major source of mantle He is required to account for these He isotope compositions. Unlike other locations on the NAF where mantle-like He is found, it is highly unlikely that the mantle He found in MMF and Gazikoy–Saros Fault fluids is produced from present-day magmatic activity: there is no active volcanism in the region of the Sea of Marmara, and the most recent volcanic activity in Thrace and Anatolia is limited to small volume, rare, Pliocene alkali basalt lavas (Pe-Piper and Piper, 2007), the closest to the fault lying 35 km to the NW. The fact that this He is not derived from active magmatism is further supported by the low temperatures of the vent fluids: these are not hydrothermal systems associated with recent intrusion of hot magma. This contrasts with the observations of Gulec et al. (2002) along subaerial portions of the NAF which show a close association between extent of mantle He contribution and the age of tectono-magmatic activity in much higher enthalpy fluids.

In summary, the He found at BB and Tekirdag is derived either directly from the mantle via high permeability pathways through the lower crust or else there is a crustal reservoir of ‘fossil’ He that is fortuitously sampled by the fault fluids. These possibilities are discussed in turn below.

5.1. A ‘fossil’ He source

Sources of ‘fossil’ He consist of mantle He that has been transferred into the crust and stored under high ${}^3\text{He}/(\text{U}+\text{Th})$ conditions, thereby creating a reservoir in the crust which preserves its initial ${}^3\text{He}/{}^4\text{He}$ ratio. Ancient magmatism which could have mobilized He from the mantle was then trapped by subsequent crystallization in the crust.

It is possible to model the evolution of ${}^3\text{He}/{}^4\text{He}$ in a ‘fossil’ intrusion (Fig. 3). However, constraining $\text{U}+\text{Th}/{}^3\text{He}$ is not straightforward, as this depends on the nature of the intrusion and few pertinent data are available. $\text{U}+\text{Th}/{}^3\text{He}$ data are available for differentiated (gabbroic) crustal intrusions which could be considered as potential analogs for differentiated crust (Moreira et al., 2003). However, these intrusions are enriched in $\text{U}+\text{Th}$ and depleted in ${}^3\text{He}$, therefore ${}^3\text{He}/{}^4\text{He}$ rapidly falls to values lower than those found at Boris’ Bubblers, and cannot be considered as potential candidates for a “fossil” He supply for BB fluids (Fig. 3). By contrast, there is a lack of suitable data on ultramafic intrusions (which are more likely to preserve high ${}^3\text{He}/{}^4\text{He}$ ratios); literature values for the average ${}^3\text{He}$ concentrations (Matsumoto et al., 2001) combined with $\text{U}+\text{Th}$ concentrations (in a separate publication (Malaviarachchi et al., 2010)) from the Horroman Ophiolite complex, (see Fig. 3 caption) suggest that $\text{U}+\text{Th}$ decay will reduce ${}^3\text{He}/{}^4\text{He}$ ratios in this type of rock to values lower than those of BB on a ~ 10 Ma timescale. Thus it is not possible to exclude a ‘fossil’ origin for the He found at BB, i.e. He trapped in an ultramafic complex within the crust below the Sea of Marmara that may have been remobilised by the fault. Nevertheless, ‘fossil’ He seems an unlikely source of the high ${}^3\text{He}/{}^4\text{He}$ found at BB: first, the limited amount of He in such a reservoir could only supply He for very short periods; secondly there is no known candidate intrusion in the immediate vicinity; and thirdly, there is no suitable mechanism for extracting significant amounts of He from cold crystallized rocks.

An alternative source of fossil, high ${}^3\text{He}/{}^4\text{He}$ helium, could be CO_2 reservoirs containing mantle derived ${}^3\text{He}$. An example has been reported from the southwestern USA (Gilfillan et al., 2009; Holland and Ballentine, 2006; Sherwood Lollar et al., 1997), which likely represents the volatiles degassed from magmas and which were subsequently trapped in impermeable traps. Such a reservoir, if intersected by the MMF, could also provide a source of

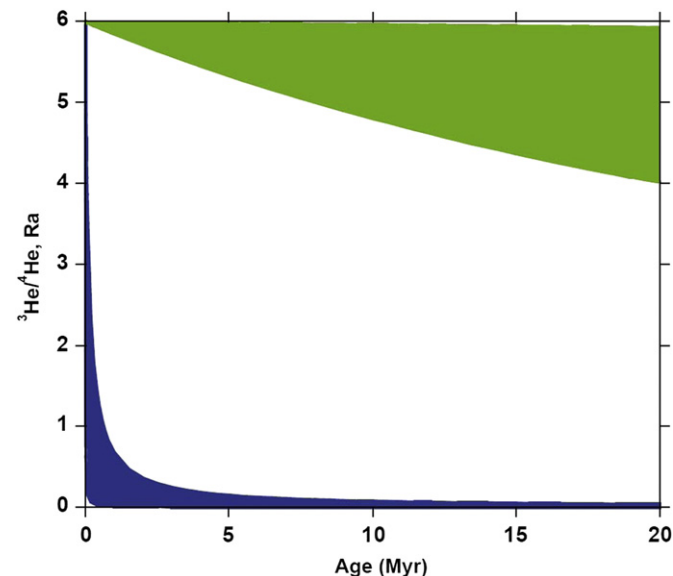


Fig. 3. Evolution of the ${}^3\text{He}/{}^4\text{He}$ ratio of a fossil pluton over time. The model assumes that a mantle-derived intrusion is placed in the crust over time. Blue=gabbroic intrusion, green=ultramafic intrusion. $(\text{U}+\text{Th})/{}^3\text{He}$ of lower crustal gabbros from (Moreira et al., 2003). $(\text{U}+\text{Th})/{}^3\text{He}$ of ultramafic intrusions is not directly known (there are few or no analyses of U, Th and He on the same samples) so we combine the He data of Matsumoto et al. (2001) and the U, Th data of Malaviarachchi et al. (2010). However, we note that ${}^3\text{He}$ concentrations of peridotites may not be representative as noble gas geochemists select He-rich samples (most rich in fluid and/or melt inclusions) for analysis and U+Th analyses do not take into account trace phases (zircon, apatite, interstitial glass). For the above reasons, it seems more likely that a real system is best represented by the lower bound of the green shaded area and may even fall below this curve. (For interpretation of the references to color in this figure legend, the reader is referred to the web version of this article.)

high ${}^3\text{He}/{}^4\text{He}$ ‘fossil’ He. While difficult to completely exclude this possibility, it nevertheless seems an unlikely source of the MMF He as there are no documented CO_2 reservoirs in the world with ${}^3\text{He}/{}^4\text{He} > 4 \text{ Ra}$.

5.2. Direct injection of mantle He into the MMF

A high permeability connection to the mantle seems the most plausible explanation for the non-radiogenic He sampled along the MMF. The subcontinental lithospheric mantle (SCLM) is generally characterized by ${}^3\text{He}/{}^4\text{He}$ slightly more radiogenic than that of the asthenospheric mantle (Gautheron and Moreira, 2002): 6 Ra is used here as the mantle source of these fluids.

Lower ${}^3\text{He}/{}^4\text{He}$ ratios measured in MMF fluids than those of the mantle are the result of (a) mixing with ${}^4\text{He}$ -rich crustal fluids and (b) ‘aging’ of the fluid during transit through the crust, where decay of U and Th in the (permeable) host rock adds ${}^4\text{He}$ to mantle-derived He. In the latter case, the change in ${}^3\text{He}/{}^4\text{He}$ ratio is a function of the U, Th content of the host lithology, of the efficiency of extracting this ${}^4\text{He}$ into the fluid and the time required to transit the crust. The general equation for transport of diluted isotopes considering only the vertical dimension and neglecting dispersion can be expressed at steady-state as (Johnson and DePaolo, 1997)

$$\nu \frac{dr_f}{dz} = \frac{J}{C_f} (r_c - r_f)$$

where ν is the average fluid velocity (mm yr^{-1}), r_f and r_c are ${}^3\text{He}/{}^4\text{He}$ ratios in the fluid and the crust, J is the “reaction flux”, the mass of He delivered to a unit volume fluid per unit time ($\text{mol m}^{-3} \text{yr}^{-1}$). C_f is the initial concentration of ${}^4\text{He}$ in the fluid

(mol m⁻³) which is calculated from the following equation:

$$C_f = \frac{[{}^3\text{He}]_f}{r_f}$$

where $[{}^3\text{He}]_f$ is the final ${}^3\text{He}$ concentration in the fluid, i.e. that was measured at the surface. Solving this equation between the surface (with the measured isotope ratio r_m) and the crust–mantle boundary (mantle isotope ratio r_M) and assuming that, relative to r_M , r_c is negligible (~ 0.02 Ra (Ballentine and Burnard, 2002; Oxburgh and O’Nions, 1987)) yields

$$\frac{1}{r_m} - \frac{1}{r_M} = \frac{JH}{v[{}^3\text{He}]}$$

where H is the vertical crustal thickness traversed by the fluid. The concentration of ${}^3\text{He}$ in the fluid is assumed to be conservative (no gains and no losses) and is known from the analyses of fault fluids. J can be expressed as a function of the crustal ${}^4\text{He}$ production rate, $P_{4\text{He}}$, normalized to a unit mass of rock ($P_{4\text{He}}$ units are mol kg⁻¹ yr⁻¹):

$$J = \frac{P_{4\text{He}} \rho_c}{V_f/V_c}$$

In this formulation, the ratio V_f/V_c is the ratio of the volume of fluid receiving the reaction products (${}^4\text{He}$) from the volume of rock V_c contributing its ${}^4\text{He}$. The maximum possible value of this ratio is that of the rock porosity ϕ . ρ_c is the crust density.

In Fig. 4, we estimate the average fluid flow velocity within the fault to be between 1 and 100 mm yr⁻¹ for BB, with flow rates 10 times faster than those calculated for other sites along the NAF (e.g. 1664–3=10–1000 mm yr⁻¹) because, although these fluids have lower ${}^3\text{He}/{}^4\text{He}$ ratios than BB fluids, they are also characterized by lower He concentrations (Table 2) and are therefore more sensitive to ${}^4\text{He}$ ingrowth. The flow rates estimated for the MMF are comparable to those of the San Andreas Fault (1–10 mm yr⁻¹ (Kennedy et al., 1997)). Fluid flow rates in both instances may be

faster than those calculated here as mixing of crustal fluids may have further lowered the ${}^3\text{He}/{}^4\text{He}$ ratio.

For a fluid flow rate of 1–100 mm yr⁻¹ with ${}^3\text{He}$ concentrations of $\approx 5 \times 10^{-13}$ mol g⁻¹ fluid for BB, the implied ${}^3\text{He}$ flux through the MMF is of the order 10^{-15} – 10^{-13} mol ${}^3\text{He}$ mm⁻² of fault yr⁻¹. Given the likely crustal thickness in this region is of the order 25 km (Becel et al., 2010), fluid residence times of 0.25–25 Ma are implied. At the slow end, the implied residence times are longer than the age of the fault itself (< 5 Ma (Armijo et al., 2005; Sengör et al., 2005)). However, the fluid migration pathways are not necessarily related to the present-day fault geometry therefore slow fluid migration remains a plausible hypothesis: prior to initiation of the NAF, the Marmara region was characterized by a large shear zone, inherited from the Intra-Pontide Suture Zone, called the ‘North Anatolian Shear Zone’ (Sengör et al., 2005). Faults within the pre-existing shear zone, which was transtensional here (Sengör et al., 2005) could thus have provided pathways for migration of mantle He bearing fluids.

5.3. Amagmatic extraction of He from the solid mantle

While the flow rates calculated above can account for how mantle-derived He can traverse the crust, the problem remains on how He can be transferred from the mantle into a fluid phase: a mechanism that releases He from the solid mantle is required.

Simple diffusion of He from peridotite with typical bulk mantle ${}^3\text{He}$ concentrations into the fault is unlikely to be sufficiently rapid to maintain the flux of mantle He estimated above. The characteristic He diffusion lengthscale ($=\sqrt{(Dt)}$) at 800 °C is of the order 1 mm yr⁻¹ ($D_{\text{He}}=2 \times 10^{-9}$ cm² s⁻¹ (Shuster et al., 2004); other estimates of D_{He} are even slower (Trull and Kurz, 1993)); given a likely mantle ${}^3\text{He}$ concentration of $\approx 9 \times 10^8$ atoms g⁻¹ (Porcelli and Elliott, 2008), the implied diffusion flux is $\sim 5 \times 10^{-19}$ mol mm⁻² of fault yr⁻¹, at least three orders of magnitude lower than the ${}^3\text{He}$ flux calculated for BB. Frictional heating during fault slip has a limited effect (e.g. $\sqrt{(Dt)}$ at 1200 °C ~ 2 mm yr⁻¹). Thus, either He is released from a larger volume of mantle than that accessible via diffusion (e.g. by alteration or by melting) and/or the mantle source has higher ${}^3\text{He}$ concentrations than ‘average’ mantle. These possibilities are investigated in turn below.

Serpentinising the overlying mantle wedge will liberate mantle He from the wedge without melting (Umeda et al., 2007a) but requires a suitable source of hydrated material. Active subduction did occur in this region before the earliest Eocene (Sengör and Yilmaz, 1981). Although this slab could have been hydrating the mantle in the region for some time since the Eocene, clearly this is a different tectonic situation from arc situations where significant quantities of recently subducted water are available for serpentinisation. Serpentinisation was probably less important in releasing mantle He in the Marmara area than in Japan, for example, nevertheless serpentinisation cannot be completely excluded as a potential mechanism for extracting mantle He.

Frictional melting in deep faults is well documented in ultramafic massifs (Andersen and Austrheim, 2006; Souquiere and Fabbri, 2010; Ueda et al., 2008). From field observations of pseudotachylite, Andersen and Austrheim (2006) estimate that 60 kg m⁻² of peridotite can be melted during co-seismic displacement. Assuming 100% melting, and that this melt completely degasses its He, then 60 kg of molten mantle produces of the order 1×10^{-12} mol ${}^3\text{He}$ m⁻² of fault. Thus if ${}^3\text{He}$ was extracted by frictional melting (mantle ${}^3\text{He}$ concentration from above), then $\sim 10^3$ slip events per year are required to account for the ${}^3\text{He}$ flux calculated for the MMF. This seems one or two orders of magnitude too high to be a realistic He extraction method.

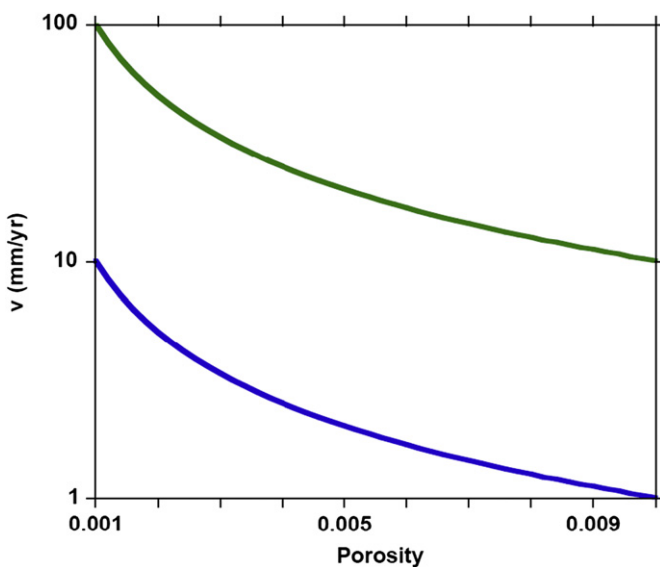


Fig. 4. Flow rate as a function of porosity for the range in [U+Th] likely for fluids traversing the crust in the MMF, calculated for the fluids emanating from Boris’ Bubblers. Blue: flow rates for [U]crust=0.25 ppm; green: flow rates for [U]crust=2.5 ppm (Th/U=4 for both cases) (Ballentine and Burnard, 2002). The connected network porosity available for fluid flow (the porosity relevant here) is difficult to constrain, depending on the wetting properties of the fluids as well as the rock fabric; we modeled fluid velocities for porosities ranging between 0.001 and 0.01 (Hyndman and Shearer, 1989).

Notwithstanding uncertainties in mantle ${}^3\text{He}$ concentrations and of the fault ${}^3\text{He}$ flux, there are difficulties maintaining the ${}^3\text{He}/{}^4\text{He}$ ratios in the MMF via diffusive extraction, alteration of the mantle or by melting during slip events.

One partial solution to the difficulty maintaining the fault He flux could be that noble gases appear to be concentrated in deformed regions of mantle. Kurz et al. (2009) show that mylonitic zones at the crust–mantle boundary have He concentrations ~10 times higher than ‘average’ mantle. Thus diffusion of ${}^3\text{He}$ out of mylonitized mantle could account for a ${}^3\text{He}$ flux of $\approx 10^{-17} \text{ mol mm}^{-2} \text{ yr}^{-1}$, approaching the ${}^3\text{He}$ fluxes observed on the MMF and on the SAF. Mylonitised zones up to several kms wide have been observed (Hekinian et al., 2000), and mylonite zones are likely stable on the 10^8 – 10^9 year timescale (Evans et al., 2001) suggesting there could be sufficient He accumulated in mylonite zones to furnish faults with high ${}^3\text{He}/{}^4\text{He}$ helium. Long-duration ($1\text{--}5 \times 10^8$ yr) deformation in the mantle, such as possible along subduction zones, could produce noble gas enriched zones which then supply the helium found in deep-rooted faults such as the NAF and SAF.

5.4. Major gas compositions

The gases escaping the MMF consist of methane, even at BB where ~70% of the He is mantle derived. While reduced C species in the mantle are known, these are restricted to subduction environments where serpentinisation has increased f_{H_2} (Song et al., 2009); in general the dominant C species in mantle derived fluids is CO_2 or CO_3^{2-} (Blundy et al., 1991; Dasgupta and Hirschmann, 2006; Zhang and Duan, 2009). Thus it seems more likely that the mantle injected CO_2 into the fault and some process or processes has either reduced the CO_2 to methane and/or added sufficient CH_4 to mask the mantle CO_2 . The fluid emitted from the mantle will be CO_2 -dominated with a $\text{CO}_2/{}^3\text{He}$ ratio of the order 2×10^9 , a ratio which is likely to be applicable to the SCLM (Fischer et al., 2009; Marty and Jambon, 1987).

Other localities also report high ${}^3\text{He}/{}^4\text{He}$ ratios in methane dominated fluids, for example Fondachello, Sicily with ${}^3\text{He}/{}^4\text{He} = 6\text{--}7 \text{ Ra}$ (Caracausi et al., 2003) and Golygina (Kamchatka) with ${}^3\text{He}/{}^4\text{He} = 5.3 \text{ Ra}$ (Taran, 2009) and both with >90% CH_4 . Fluids emanating from the extensional Pannonian and Vienna basins have a wide range of CO_2/CH_4 ratios with some methane rich fluids that are associated with ${}^3\text{He}/{}^4\text{He}$ as high as 2.3 Ra (Sherwood Lollar et al., 1997). These fluid compositions result from CO_2 loss (by dissolution in water and/or precipitation of carbonate) combined with methane addition from within the basin. Alternatively, CO_2 -bearing mantle fluids could be directly reduced to CH_4 either microbially (Greenbaum et al., 1995) or, under specific conditions, inorganically via Fischer–Tropsch type reactions (Foustoukos and Seyfried Jr, 2004; Holm and Charlou, 2001; McCollom and Seewald, 2006; Taran et al., 2007).

However, it is not necessary to invoke CO_2 -consuming reactions to explain the MMF data: simple mixing between CO_2 dominated mantle fluids and CH_4 crustal fluids can generate the range in ${}^3\text{He}/{}^4\text{He}$ – CH_4/CO_2 compositions analyzed here. Fig. 5 shows the likely compositions of mixtures of mantle fluids (CO_2 dominated) and methane produced in a sedimentary basin; mixing between these two fluids is highly probable in a situation such as the Marmara Sea where fluids of mantle origin percolate through young, organic rich sediments.

Thus it is possible to reproduce the compositions found along the NAF (including the high ${}^3\text{He}/{}^4\text{He}$, methane dominated fluids found at BB) simply by mixing, provided $(\text{CH}_4/{}^4\text{He})_{\text{mantle}} \ll (\text{CH}_4/{}^4\text{He})_{\text{crust}}$. $(\text{CH}_4/{}^4\text{He})_{\text{mantle}}$ is low, between 0.1 and 0.2 (Javoy and Pineau, 1991). Then $\text{CH}_4/{}^4\text{He}$ of the basin fluid higher than ≈ 100 would result in the appropriate ‘r’ value (Langmuir et al.,

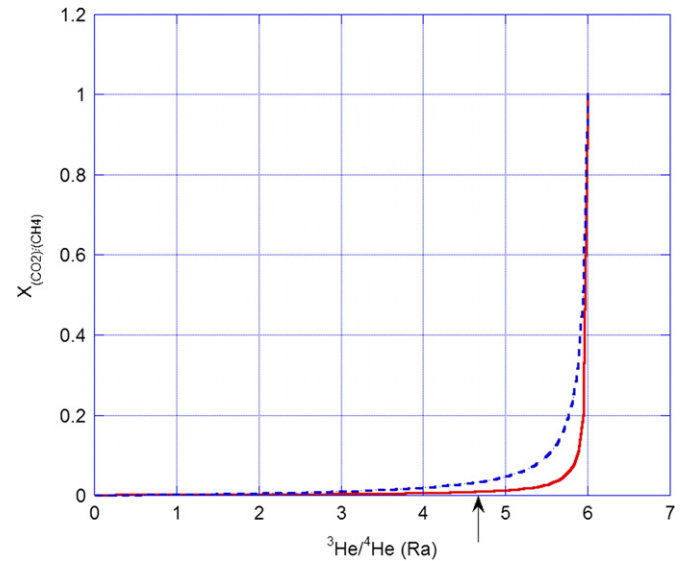


Fig. 5. Predicted fluid He isotope ratios as a function of the partial molar CO_2 content ($X_{\text{CO}_2/\text{CH}_4}$) during mixing between methane-rich basin fluids and a typical mantle fluid. No consumption or production of either fluid is assumed. The endmember compositions assumed for the model are $({}^3\text{He}/{}^4\text{He})_{\text{mantle}} = 6 \text{ Ra}$, $(X_{\text{CO}_2}/X_{\text{CH}_4})_{\text{mantle}} = 0.999$ and $({}^3\text{He}/{}^4\text{He})_{\text{crust}} = 0.02 \text{ Ra}$, $(X_{\text{CO}_2}/X_{\text{CH}_4})_{\text{crust}} = 0.001$. In this diagram, the curvature of the mixing line, r , depends on the ratio $(\text{CH}_4/{}^4\text{He})_{\text{mantle}}/(\text{CH}_4/{}^4\text{He})_{\text{crust}}$ which is varied between 0.01 (blue, dashed) and 0.0025 (red, solid). The arrow shows the ${}^3\text{He}/{}^4\text{He}$ composition analyzed for Boris' Bubblers (4.9 Ra). Thus, an ‘r’ value of 0.01 would predict 4% mantle derived CO_2 in the Boris' Bubblers fluid while ‘r’ = 0.0025 would have only 1% mantle derived CO_2 , consistent with the fluid compositions. (For interpretation of the references to color in this figure legend, the reader is referred to the web version of this article.)

1978) (see Fig. 5 caption). Typical natural gas accumulations have $\text{CH}_4/{}^4\text{He}$ ratios in the range of 600–8000 (Battani et al., 2000); young sedimentary basins (such as the Sea of Marmara) will be expected to be at the upper end of this range considering that the $\text{CH}_4/{}^4\text{He}$ ratio of the basin fluids will decrease with time as ${}^4\text{He}$ is produced by U-series decay. Finally, this is borne out by the high $\text{CH}_4/{}^4\text{He}$ ratios in sample 1662-2 (1.5×10^6 ; Table 2), consistent with the C/He ratio of hydrocarbons generated from young sedimentary basins (Prinzhofner et al., 2010).

The C/ ${}^3\text{He}$ compositions of the three samples of Boris' Bubblers are highly variable (Fig. 6, Table 2). This 10^3 variation in C/He is difficult to explain, given that the fluids were collected within a short space of time (few hours) and short distances (<50 m) of each other. Although this may be a sampling artifact (preferential He loss from the Cu tubes), the heterogeneity could also be due to shallow level advection of basin derived methane, or possibly due to production or consumption of CH_4 by microbial communities living in the vents of Boris' Bubblers.

Although we cannot exclude mechanisms where mantle CO_2 is consumed (bacterially or inorganically), these mechanisms are not *a priori* necessary to explain the data (Fig. 5 caption). Dilution of mantle-derived CO_2 rich fluids by CH_4 produced within the basin further seems likely as C/ ${}^3\text{He}$ ratios are roughly correlated with the fluid's ${}^3\text{He}/{}^4\text{He}$ (Fig. 6), demonstrating that the C (or methane) rich endmember also carries ${}^4\text{He}$. It seems probable therefore that mantle derived CO_2 (with accompanying He) percolated through the fault to shallow levels where it was diluted by CH_4 produced by thermal and bacterial degradation of young, organic rich sediments in the Marmara Basin.

6.5. Potential for fault weakening by mantle-derived fluids

The NAF in Anatolia represents a weak heterogeneity in the local lithosphere and is therefore a “weak” fault (Provost et al.,

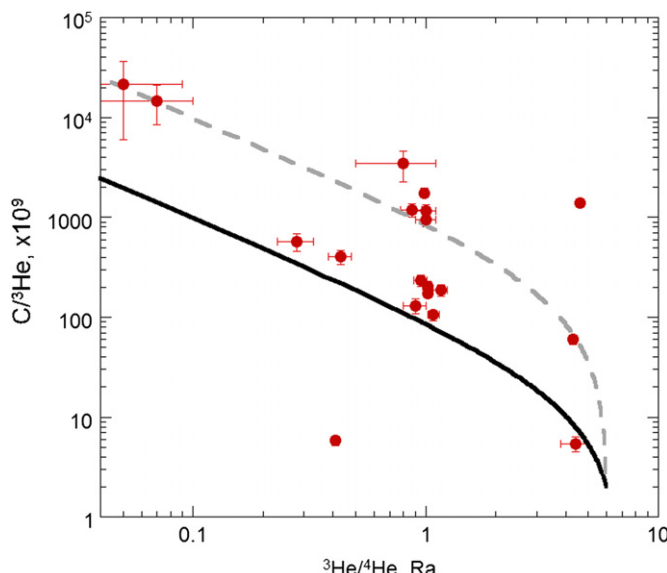


Fig. 6. ${}^3\text{He}/{}^4\text{He}$ and $\text{C}/{}^3\text{He}$ relationship for Marmara fluids. The association of low ${}^3\text{He}/{}^4\text{He}$ ratios with high $\text{C}/{}^3\text{He}$ is consistent with addition of methane (probably thermogenic in origin (Bourry et al., 2009) but with high C/He ratios, as would be expected in a young sedimentary basin) to mantle derived gases. Mixing between hypothetical endmembers that have the same mantle pole composition (${}^3\text{He}/{}^4\text{He}=6 \text{ Ra}$, $\text{C}/{}^3\text{He}=2 \times 10^9$) but different basin fluid compositions are shown (dashed line: ${}^3\text{He}/{}^4\text{He}=0.01 \text{ Ra}$; $\text{C}/{}^3\text{He}=1 \times 10^{14}$; solid line: ${}^3\text{He}/{}^4\text{He}=0.01 \text{ Ra}$, $\text{C}/{}^3\text{He}=1 \times 10^{13}$). The poor correlation is expected as the basin-produced methane likely has variable ${}^4\text{He}$ content, depending on the age and U+Th content of the source rocks.

2003), as is the SAF (Lachenbruch and Sass, 1980). Similarly to the SAF, the NAF GPS velocity field is best replicated using friction coefficients of 0.05 (with an upper limit of 0.1); the fault would be locked for friction coefficients > 0.2 . More recently, (Hergert and Heidbach, 2010; Hergert et al., 2011) concluded that friction coefficients of the order 0.05 would be consistent with measured fault velocities in the region studied here. It seems most likely that the major faults in the Sea of Marmara and vicinity are likewise “weak”.

High pressure fluids localized on the fault planes have been invoked to reduce the effective shear stress required for slip (Faulkner and Rutter, 2001; Hickman et al., 1995). Mantle derived fluids – H_2O and CO_2 – potentially provide a mechanism for weakening strike-slip faults. It seems unlikely, however, that these could be responsible for fault weakening on the MMF. First, even where mantle He has been identified (e.g. Boris’ Bubblers), the majority of the fluid flux is methane (and presumably entrained water) of shallow origin which cannot contribute to fault lubrication within the crystalline crust. Secondly, it is notable that the principal site of mantle He emanation along the entire length of the NAF is the Boris’ Bubblers site where the MMF is intersected by a normal fault (Tary et al., 2011) while elsewhere along the NAF, high ${}^3\text{He}/{}^4\text{He}$ fluids are associated with recent magmatic activity and therefore are probably not due to fault-related fluids (Gulec et al., 2002). In addition, the BB location falls on a fault intersection associated with higher permeability, thereby increasing fluid advection along this part of the fault: this location cannot be considered to be representative of fault conditions for the MMF or NAF in general (Tary et al., 2011). A similar observation can be made for the SAF: there is only a single site on the SAF that has $> 50\%$ mantle He (Mersey Hot Spring), and this site is also associated with a splay fault. The Mersey Hot Spring site is located on the Tesla–Ortigalita fault, a reactivated extensional structure (Fuis and Mooney, 1990).

Thus it seems that although mantle He can be advected along fault planes, this phenomenon is limited to very specific strain situations and is not necessarily a general feature of strike-slip faulting, an observation supported by analyses of He isotopes in deep fluids from the San Andreas Fault Observatory at Depth (SAFOD) drill core, where less than 5% of the helium at depth originates from the mantle (Wiersberg and Erzinger, 2007). Therefore it is difficult to invoke mantle fluids as rheology modifiers during faulting in compressional environments.

6. Conclusions

Mantle derived He is clearly present in fluids emanating from the Marmara Main Fault, accounting for between $< 5\%$ and $\sim 70\%$ of the He. By contrast, the gases themselves are dominated by CH_4 . Dilution of CO_2 -rich mantle fluids by CH_4 generated in the basin itself (which is likely to have very high $\text{CH}_4/{}^4\text{He}$ ratios) could account for the compositions observed: CO_2 consuming mechanisms are not needed to account for the data, although such mechanisms cannot be excluded either. Nevertheless, mixing between mantle derived and basin derived fluids has occurred, resulting in a negative correlation between $\text{C}/{}^3\text{He}$ and ${}^3\text{He}/{}^4\text{He}$ in the fault fluids.

The highest ${}^3\text{He}/{}^4\text{He}$ ratios (highest mantle He contribution) is found at the intersection between the MMF and a splay fault with a normal component. It seems likely that the change in strain regime (from predominantly compressive along the majority of the MMF to strike slip with a normal component (Tary et al., 2011)) determines the fault permeability.

It is possible to constrain the vertical fluid velocity within the fault from the change in He isotope composition if the rate of ${}^4\text{He}$ production in the crust and the efficiency of transferring this He into the fault itself are known (Kennedy et al., 1997). It is likely that He in the fault has a vertical velocity of between 1 and 100 mm yr^{-1} , corresponding to a ${}^3\text{He}$ flux of the order 10^{-13} – 10^{-15} mol $\text{mm}^{-2} \text{ yr}^{-1}$. Melting induced by frictional heating and/or serpentinisation are potential mechanisms for releasing He from the solid mantle.

Acknowledgments

The captain and crew of the R/V Atalante and all who made sampling in the Sea of Marmara possible are warmly thanked for their considerable efforts on our behalf. Financial support to M. Tryon was provided by NSF Award no. OCE-0647361. Two anonymous reviewers are thanked for their reviews and Yuri Taran is particularly thanked for discussions and comments during the review process. This is CRPG contribution number 2159.

Appendix A. Supporting information

Supplementary data associated with this article can be found in the online version at <http://dx.doi.org/10.1016/j.epsl.2012.05.042>.

References

- Ambraseys, N.N., Jackson, J.A., 2000. Seismicity of the Sea of Marmara (Turkey) since 1500. *Geophys. J. Int.* 141, F1–F6.
- Andersen, T.B., Austrheim, H., 2006. Fossil earthquakes recorded by pseudotachylites in mantle peridotite from the Alpine subduction complex of Corsica. *Earth Planet. Sci. Lett.* 242, 58–72.
- Armijo, R., Pondard, N., Meyer, B., Ucarkus, G., de Lepinay, B.M., Malavieille, J., Dominguez, S., Gustcher, M.A., Schmidt, S., Beck, C., Cagatay, N., Cakir, Z.,

- Imren, L., Eris, K., Natal'in, B., Ozalbayev, S., Tolun, L., Lefevre, I., Seeber, L., Gasperini, L., Rangin, C., Emre, O., Sarikavak, K., 2005. Submarine fault scarps in the Sea of Marmara pull-apart (North Anatolian Fault): implications for seismic hazard in Istanbul. *Geochem. Geophys. Geosyst.*, 6.
- Ballentine, C.J., Burnard, P.G., 2002. Production, release and transport of noble gases in the continental crust. *Rev. Mineral. Geochem.* 47, 481–538.
- Barka, A.A., 1992. The North Anatolian Fault Zone. *Ann. Tectonicae* 6, 164–195.
- Battani, A., Sarda, P., Prinzhofner, A., 2000. Basin scale natural gas source, migration and trapping traced by noble gases and major elements: the Pakistan Indus Basin. *Earth Planet. Sci. Lett.* 181, 229–249.
- Becel, A., Laigle, M., de Voogd, B., Hirn, A., Taymaz, T., Yolsal-Cevikbilen, S., Shimamura, H., et al., 2010. North Marmara Trough architecture of basin infill, basement and faults, from PSDM reflection and OBS refraction seismics. *Tectonophysics* 490, 1–14.
- Blundy, J.D., Brodholt, J.P., Wood, B.J., 1991. Carbon–fluid equilibria and the oxidation state of the upper mantle. *Nature* 349, 321–324.
- Bourry, C., Chazallon, B., Charlou, J.L., Pierre Donval, J., Ruffine, L., Henry, P., Gelli, L., Çagatay, M.N., Inan, S., Moreau, M., 2009. Free gas and gas hydrates from the Sea of Marmara, Turkey: chemical and structural characterization. *Chem. Geol.* 264, 197–206.
- Brauer, K., Kampf, H., Strauch, G., 2009. Earthquake swarms in non-volcanic regions: what fluids have to say. *Geophys. Res. Lett.*, 36.
- Caracausi, A., Italiano, F., Paonita, A., Rizzo, A., 2003. Evidence of deep magma degassing and ascent by geochemistry of peripheral gas emissions at Mount Etna (Italy): assessment of the magmatic reservoir pressure. *J. Geophys. Res. B: Solid Earth*, B10.
- Coskun, B., 1997. Oil and gas fields—transfer zone relationships, Thrace basin, NW Turkey. *Mar. Pet. Geol.* 14, 401–416.
- Coskun, B., 2000. North Anatolian Fault–Saros Gulf relationships and their relevance to hydrocarbon exploration, northern Aegean Sea, Turkey. *Mar. Pet. Geol.* 17, 751–772.
- Crossey, L., Karlstrom, K., Springer, A., Newell, D., Hilton, D.R., Fischer, T., 2009. Degassing of mantle-derived CO₂) and He from springs in the southern Colorado Plateau region—Neotectonic connections and implications for groundwater systems. *Geol. Soc. Am. Bull.* 121, 1034–1053.
- Dasgupta, R., Hirschmann, M.M., 2006. Melting in the Earth's deep upper mantle caused by carbon dioxide. *Nature* 440, 659–662.
- de Leeuw, G.A.M., Hilton, D.R., Gulec, N., Mutlu, H., 2010. Regional and temporal variations in CO₂/³He, ³He/⁴He and δ¹³C along the North Anatolian Fault Zone, Turkey. *Appl. Geochem.* 25, 524–539.
- Dogan, T., Sumino, H., Nagao, K., Notsu, K., Tuncer, M.K., Celik, C., 2009. Adjacent releases of mantle helium and soil CO₂ from active faults: observations from the Marmara region of the North Anatolian Fault zone, Turkey. *Geochem. Geophys. Geosyst.*, 10.
- Ercan, T., Matsuda, J., Nagao, K., Kita, I., 1995. Noble gas isotopic compositions in gas and water samples from Anatolia. In: Erler, A., Ercan, T., Bingöl, E., Örçen, S. (Eds.), *Geology of the Black Sea Region: Proceedings of the International Symposium on the Geology of the Black Sea Region*, pp. 197–206.
- Evans, B., Renner, J., Hirth, G., 2001. A few remarks on the kinetics of static grain growth in rocks. *Int. J. Earth Sci.* 90, 88–103.
- Faulkner, D.R., Rutter, E.H., 2001. Can the maintenance of overpressured fluids in large strike-slip fault zones explain their apparent weakness? *Geology* 29, 503–506.
- Fischer, T., Burnard, P., Marty, B., Hilton, D.R., Furi, E., Palhol, F., Sharp, Z.D., 2009. Volcanic gas chemistry from the erupting Ol doinyo Lengai (East Africa): origin of carbonatite magmas. *Nature* 459, 77–80.
- Foustoukos, D.I., Seyfried Jr, W.E., 2004. Hydrocarbons in hydrothermal vent fluids: the role of chromium-bearing catalysts. *Science* 304, 1002–1005.
- Fuis, G.S., Mooney, W.D., 1990. Lithospheric structure and tectonics from seismic-refraction and other data. In: Wallace, R.E. (Ed.), *The San Andreas Fault System, California*, pp. 283, US Geological Survey Professional Paper 1515.
- Gautheron, C., Moreira, M., 2002. Helium signature of the subcontinental lithospheric mantle. *Earth Planet. Sci. Lett.* 199, 39–47.
- Géli, L., Henry, P., Zitter, T., Dupré, S., Tryon, M., Çagatay, M.N., de Lépinay, B.M., Le Pichon, X., Sengör, A.M.C., Görür, N., Natal'in, B., Uçarkuş, G., Özerner, S., Volker, D., Gasperini, L., Burnard, P., Bourlange, S., Party, t.M.S., 2008. Gas emissions and active tectonics within the submerged section of the North Anatolian Fault zone in the Sea of Marmara. *Earth Planet. Sci. Lett.* 274, 34–39.
- Gherardi, F., Panichi, C., Gonfiantini, R., Magro, G., Scandiffio, G., 2005. Isotope systematics of C-bearing gas compounds in the geothermal fluids of Larderello, Italy. *Geothermics* 34, 442–470.
- Gilliland, S.M.V., Lollar, B.S., Holland, G., Blagburn, D., Stevens, S., Schoell, M., Cassidy, M., Ding, Z., Zhou, Z., Lacrampe-Couloume, G., Ballentine, C.J., 2009. Solubility trapping in formation water as dominant CO₂ sink in natural gas fields. *Nature* 458, 614–618.
- Goncuoglu, M.C., Turhan, N., Senturk, K., Ozcan, A., Uysal, S., Yaliniz, M.K., 2000. A geotraverse across northwestern Turkey: tectonic units of the Central Sakarya region and their tectonic evolution. *Geological Society Special Publication*, 139–161.
- Greenbaum, E., Lee, J.W., Tevault, C.V., Blankinship, S.T., Mets, L.J., 1995. CO₂ fixation and photoevolution of H₂ and O₂ in a mutant of chlamydomonas lacking photosystem. *Nature* 376, 438–441.
- Gulec, N.H., Hilton, D.R., 2006. Helium and heat distribution in western Anatolia, Turkey: Relationship to active extension and volcanism. In: Dilek, Y., Pavlides, S., (Eds.), *Postcollisional Tectonics and Magmatism in the Mediterranean Region and Asia*. In: *Geological Society of America Special Papers*, Vol. 409, pp. 305–319. [http://dx.doi.org/10.1130/2006.2409\(16\)](http://dx.doi.org/10.1130/2006.2409(16)).
- Gulec, N., Hilton, D.R., Mutlu, H., 2002. Helium isotope variations in Turkey: relationship to tectonics, volcanism and recent seismic activities. *Chem. Geol.* 187, 129–142.
- Gürgey, K., 2009. Geochemical overview and undiscovered gas resources generated from Hamitabat petroleum system in the Thrace Basin, Turkey. *Mar. Pet. Geol.* 26, 1240–1254.
- Gürgey, K., Philp, R., Clayton, C., Emiro lu, H., Siyako, M., 2005. Geochemical and isotopic approach to maturity/source/mixing estimations for natural gas and associated condensates in the Thrace Basin, NW Turkey. *Appl. Geochem.* 20, 2017–2037.
- Hekinian, R., Juteau, T., Gracia, E., Sichler, B., Sichel, S., Udintsev, G., Apprioual, R., Ligi, M., 2000. Submersible observations of equatorial atlantic mantle: the St. Paul Fracture Zone region. *Mar. Geophys. Res.* 21, 529–560.
- Hergert, T., Heidbach, O., 2010. Slip-rate variability and distributed deformation in the Marmara Sea fault system. *Nat. Geosci.* 3, 132–135.
- Hergert, T., Heidbach, O., Becel, A., Laigle, M., 2011. Geomechanical model of the Marmara Sea region—I. 3-D contemporary kinematics. *Geophys. J. Int.* 185, 1073–1089.
- Hickman, S., Sibson, R., Bruhn, R., 1995. Mechanical involvement of fluids in faulting. *J. Geophys. Res. B: Solid Earth* 100, 12831–12840.
- Holland, G., Ballentine, C.J., 2006. Seawater subduction controls the heavy noble gas composition of the mantle. *Nature* 441, 186–191.
- Holm, N.G., Charlou, J.L., 2001. Initial indications of abiotic formation of hydrocarbons in the Rainbow ultramafic hydrothermal system, Mid-Atlantic Ridge. *Earth Planet. Sci. Lett.* 191, 1–8.
- Holzner, C.P., McGinnis, D.F., Schubert, C.J., Kipfer, R., Imboden, D.M., 2008. Noble gas anomalies related to high-intensity methane gas seeps in the Black Sea. *Earth Planet. Sci. Lett.* 265, 396–409.
- Hosgörmez, H., Yalçın, M.N., Cramer, B., Gerling, P., Mann, U., 2005. Molecular and isotopic composition of gas occurrences in the Thrace basin (Turkey): origin of the gases and characteristics of possible source rocks. *Chem. Geol.* 214, 179–191.
- Huvaz, O., Karahanoglu, N., Ediger, V., 2007. The thermal gradient history of the thrace basin, NW Turkey: correlation with basin evolution processes. *J. Pet. Geol.* 30, 3–24.
- Hyndman, R.D., Shearer, P.M., 1989. Water in the lower continental crust: modelling magnetotelluric and seismic reflection results. *Geophys. J. Int.* 98 (2), 343–365.
- Iio, Y., Sagiyama, T., Kobayashi, Y., Shiozaki, I., 2002. Water-weakened lower crust and its role in the concentrated deformation in the Japanese Islands. *Earth Planet. Sci. Lett.* 203, 245–253.
- Javoy, M., Pineau, F., 1991. The volatiles record of a “popping” rock from the Mid-Atlantic Ridge at 14°N: chemical and isotopic composition of gas trapped in the vesicles. *Earth Planet. Sci. Lett.* 107, 598–611.
- Jean-Baptiste, P., Charlou, J.L., Stievenard, M., Donval, J.P., Bougault, H., Mevel, C., 1991. Helium and methane measurements in hydrothermal fluids from the mid-Atlantic ridge: the Snake Pit site at 23°N. *Earth Planet. Sci. Lett.* 106, 17–28.
- Johnson, T.M., DePaolo, D.J., 1997. Rapid exchange effects on isotope ratios in groundwater systems 1. Development of a transport-dissolution-exchange model. *Water Resour. Res.* 33, 187–195.
- Kennedy, B.M., Kharaka, Y.K., Evans, W.C., Ellwood, A., De Paolo, D.J., Thordsen, J.J., Ambats, G., Mariner, R.H., 1997. Mantle fluids in the San Andreas fault system, California. *Science* 278, 1278–1281.
- Kennedy, B.M., Van Soest, M.C., 2007. Flow of mantle fluids through the ductile lower crust: helium isotope trends. *Science* 318, 1433–1436.
- Kulogoski, J.T., Hilton, D.R., Izicki, J.A., 2005. Source and movement of helium in the eastern Morongo groundwater Basin: the influence of regional tectonics on crustal and mantle helium fluxes. *Geochim. Cosmochim. Acta* 69, 3857–3872.
- Kurz, M.D., Warren, J.M., Curtice, J., 2009. Mantle deformation and noble gases: helium and neon in oceanic mylonites. *Chem. Geol.* 266, 10–18.
- Kuscu, I., Okamura, M., Matsuoka, H., Gokasan, E., Awata, Y., Tur, H., Simsek, M., Kecer, M., 2005. Seafloor gas seeps and sediment failures triggered by the August 17, 1999 earthquake in the Eastern part of the Gulf of Izmit, Sea of Marmara, NW Turkey. *Mar. Geol.* 215, 193–214.
- Lachenbruch, A.H., Sass, J.H., 1980. Heat flow and energetics of the San Andreas fault zone. *J. Geophys. Res.* 85, 6185–6223.
- Langmuir, C.H., Vocke, R.D., Hanson, G.N., Hart, S.R., 1978. A general mixing equation with applications to Icelandic basalts. *Earth Planet. Sci. Lett.* 37, 380–392.
- Malaviarachchi, S.P.K., Makishima, A., Nakamura, E., 2010. Melt-peridotite reactions and fluid metasomatism in the upper mantle, revealed from the geochemistry of peridotite and gabbro from the Horoman peridotite massif, Japan. *J. Petrol.* 51, 1417–1445.
- Marty, B., Jambon, A., 1987. C/³He in volatile fluxes from the solid Earth: implications for carbon geodynamics. *Earth Planet. Sci. Lett.* 83, 16–26.
- Matsumoto, T., Chen, Y., Matsuda, J.-i., 2001. Concomitant occurrence of primordial and recycled noble gases in the Earth's mantle. *Earth Planet. Sci. Lett.* 185, 35–47.
- McCollom, T.M., Seewald, J.S., 2006. Carbon isotope composition of organic compounds produced by abiotic synthesis under hydrothermal conditions. *Earth Planet. Sci. Lett.* 243, 74–84.
- Moreira, M., Bluszta, J., Curtice, J., Hart, S.R., Dick, H.J.B., Kurz, M.D., 2003. He and Ne isotopes in oceanic crust: implications for noble gas recycling in the mantle. *Earth Planet. Sci. Lett.* 216, 635–643.
- Moreira, M., Kunz, J., Allègre, C., 1998. Rare gas systematics in popping rock: isotopic and elemental compositions in the upper mantle. *Science* 279, 1178–1181.

- Mutlu, H., Guelec, N., Hilton, D.R., 2008. Helium–carbon relationships in geothermal fluids of western Anatolia, Turkey. *Chem. Geol.* 247, 305–321.
- Okay, A.I., Demirbag, E., Kurt, H., Okay, N., Kuscu, I., 1999. An active, deep marine strike-slip basin along the North Anatolian fault in Turkey. *Tectonics* 18, 129–147.
- Okay, A.I., Tansel, I., Tuysuz, O., 2001. Obduction, subduction and collision as reflected in the Upper Cretaceous–Lower Eocene sedimentary record of western Turkey. *Geol. Mag.* 138, 117–142.
- Oxburgh, E.R., O’Nions, R.K., 1987. Helium loss, tectonics, and the terrestrial heat budget. *Science* 237, 1583–1588.
- Pe-Piper, G., Piper, D.J.W., 2007. Neogene backarc volcanism of the Aegean: new insights into the relationship between magmatism and tectonics. *Geol. Soc. Am. Spec. Pap.*, 17–31.
- Perincek, D., 1991. Possible strand of the North Anatolian Fault in the Thrace Basin, Turkey—an interpretation. *Am. Assoc. Pet. Geol. Bull.* 75, 241–257.
- Porcelli, D., Elliott, T., 2008. The evolution of He isotopes in the convecting mantle and the preservation of high $^{3}\text{He}/^{4}\text{He}$ ratios. *Earth Planet. Sci. Lett.* 269, 175–185.
- Prinzhofer, A., Neto, E.V.D., Battani, A., 2010. Coupled use of carbon isotopes and noble gas isotopes in the Potiguar basin (Brazil): fluids migration and mantle influence. *Mar. Pet. Geol.* 27, 1273–1284.
- Provost, A., Chery, J., Hassani, R., 2003. 3D mechanical modeling of the GPS velocity field along the North Anatolian fault. *Earth Planet. Sci. Lett.* 209, 3610377.
- Şen, Şamil, Yillar, Selin, Kerey, Erdal, 2009. Allochthonous blocks misidentified as the basement: implication for petroleum exploration in the SW Thrace Basin (Turkey). *J. Pet. Sci. Eng.* 64, 55–66.
- Sano, Y., Wakita, H., 1985. Geographical distribution of ($\text{super } 3$) He/($\text{super } 4$) He ratios in Japan: implications for arc tectonics and incipient magmatism. *J. Geophys. Res. B* 90, 8729–8741.
- Sengör, A.M.C., Tuysuz, O., İmren, C., Sakinç, M., Eyidogán, H., Gorur, N., Le Pichon, X., Rangin, C., 2005. The North Anatolian Fault: a new look. *Annu. Rev. Earth Planet. Sci.*, 37–112.
- Sengör, A.M.C., Yilmaz, Y., 1981. Tethyan evolution of Turkey: a plate tectonic approach. *Tectonophysics* 75 (pp. 181–190, 193–199, 203–241).
- Sherwood Lollar, B., Ballentine, C.J., O’Nions, R.K., 1997. The fate of mantle-derived carbon in a continental sedimentary basin: integration of C/He relationships and stable isotope signatures. *Geochim. Cosmochim. Acta* 61, 2295–2307.
- Shuster, D.L., Farley, K.A., Sisterson, J.M., Burnett, D.S., 2004. Quantifying the diffusion kinetics and spatial distributions of radiogenic ^{4}He in minerals containing proton-induced ^{3}He . *Earth Planet. Sci. Lett.* 217, 19–32.
- Siyako, M., Huvaz, O., 2007. Eocene stratigraphic evolution of the Thrace Basin, Turkey. *Sediment. Geol.* 198, 75–91.
- Song, S., Su, L., Niu, Y., Lai, Y., Zhang, L., 2009. CH₄ inclusions in orogenic harzburgite: evidence for reduced slab fluids and implication for redox melting in mantle wedge. *Geochim. Cosmochim. Acta* 73, 1737–1754.
- Souquière, F., Fabbri, O., 2010. Pseudotachylites in the Balmuccia peridotite (Ivrea Zone) as markers of the exhumation of the southern Alpine continental crust. *Terra Nova* 22, 70–77.
- Tanaka, S.S., Watanabe, Y.W., 2007. A high accuracy method for determining nitrogen, argon and oxygen in seawater. *Mar. Chem.* 106, 516–529.
- Taran, Y., 2009. Geochemistry of volcanic and hydrothermal fluids and volatile budget of the Kamchatka–Kuril subduction zone. *Geochim. Cosmochim. Acta* 73, 1067–1094.
- Taran, Y.A., Kliger, G.A., Sebastianov, V.S., 2007. Carbon isotope effects in the open-system Fischer–Tropsch synthesis. *Geochim. Cosmochim. Acta* 71, 4474–4487.
- Tary, J.B., Geli, L., Henry, P., Natal'in, B., Gasperini, L., Comoglu, M., Cagatay, N., Bardainne, T., 2011. Sea-bottom observations from the western escarpment of the Sea of Marmara. *Bull. Seismol. Soc. Am.* 101, 775–791.
- Trull, T., Kurz, M.D., 1993. Experimental measurements of ^{3}He and ^{4}He mobility in olivine and clinopyroxene at magmatic temperatures. *Geochim. Cosmochim. Acta* 47, 1313–1324.
- Tryon, M.D., Henry, P., Çagatay, M.N., Zitter, T.A.C., Géli, L., Gasperini, L., Burnard, P., Bourlange, S., Grall, C., 2010. Pore fluid chemistry of the North Anatolian Fault zone in the Sea of Marmara: a diversity of sources and processes. *Geochem. Geophys. Geosyst.*, 11 (art. no. Q0AD03).
- Turgut, S., Eseller, G., 2000. Sequence stratigraphy, tectonics and depositional history in eastern Thrace Basin, NW Turkey. *Mar. Pet. Geol.* 17, 61–100.
- Ueda, T., Obata, M., Di Toro, G., Kanagawa, K., Ozawa, K., 2008. Mantle earthquakes frozen in mylonitized ultramafic pseudotachylites of spinel-lherzolite facies. *Geology* 36, 607–610.
- Umeda, K., McCrank, G.F., Ninomiya, A., 2007a. Helium isotopes as geochemical indicators of a serpentized fore-arc mantle wedge. *J. Geophys. Res. B: Solid Earth*, 112.
- Umeda, K., Ninomiya, A., McCrank, G.F., 2008. High ^{3}He emanations from the source regions of recent large earthquakes, central Japan. *Geochem. Geophys. Geosyst.*, 9.
- Umeda, K., Sakagawa, Y., Ninomiya, A., Asamori, K., 2007b. Relationship between helium isotopes and heat flux from hot springs in a non-volcanic region, Kii Peninsula, southwest Japan. *Geophys. Res. Lett.*, 34.
- Wiersberg, T., Erzinger, J., 2007. A helium isotope cross-section study through the San Andreas Fault at seismogenic depths. *Geochem. Geophys. Geosyst.*, 8.
- Zhang, C., Duan, Z., 2009. A model for C–O–H fluid in the Earth’s mantle. *Geochim. Cosmochim. Acta* 73, 2089–2102.
- Zitter, T.A.C., Henry, P., Aloisi, G., Delaygue, G., Çagatay, M.N., Mercier de Lepinay, B., Al-Samir, M., Fornaciari, F., Tesmer, M., Pekdeger, A., Wallmann, K., Lercolais, G., 2008. Cold seeps along the main Marmara Fault in the Sea of Marmara (Turkey). *Deep-Sea Res. Part I: Oceanogr. Res. Pap.* 55, 552–570.
- Zoback, M.D., Beroza, G.C., 1993. Evidence for near-frictionless faulting in the 1989 (M 6.9) Loma Prieta, California, earthquake and its aftershocks. *Geology* 21, 181–185.